HiSST: International Conference on
High-Speed Vehicle Science Technology
26–29 November 2018, Moscow, Russia

Investigation on Flow Characteristic of Combination of Forward-facing Jet and Spike through Wind Tunnel Tests

Jiang ZHANG[1], Xiaoyan HE[2], Handong MA[3], Yongming QIN[4]

Abstract

The flow characteristics around the blunt body with forward-facing jet and spike are investigated through wind tunnel experiments, which include the mechanism of steady mode and unsteady mode. The dynamic-force measurement, dynamic-pressure measurement and schlieren are involved. The results indicate that there are the steady mode and the unsteady mode for the flow field around the blunt body with the combination of forward-facing jet and spike. The flow is steady as the pressure ratio of the supersonic jet is higher than the critical pressure ratio, while it is under unsteady mode as the pressure ratio of the supersonic jet lower than the critical pressure ratio. The drag of the blunt body decreases with the increasing of the length of spike until the length of the spike reaches a certain value. With the enhancement of jet pressure ratio the strength of the reattached shock waves is weakened significantly, which is beneficial to eliminate the hot spot on the shoulder of blunt body. The pressure on the suface surrounded by the reattach shock waves is fluctuant intensively under the unsteady mode, which is induced by the self-excited oscillations of shock waves around the blunt body. The dominant frequency of the self-excited oscillation decreases with the increasing of jet pressure ratio. The mechanism of self-excited oscillation is that the ambient pressure around the jet exit cannot be persistently balanced when jet pressure ratio is lower than the critical pressure ratio.

Keywords: forward-facing jet, spike, wind tunnel, drag reduction, blunt body

1. Introduction

Strong bow shock wave is generated near the nose of blunt body when it cruises at supersonic or hypersonic speeds. Aerodynamic resistance increasing, air-heating, and sonic boom is caused after the shock wave. To resolve these problems, a spike [1-5] or a forward-facing jet [6-10] can be mounted on the nose of the blunt body, as a result of which the structure of the bow shocks is changed and the intensity of the bow shocks[11]is decreased. As the spike is used alone, the stagnation point is on the top of it, where the aerodynamic heating is strong, which may ablatethe spike. Furthermore, hot spots on the shoulder of blunt body may appear near the reattach shocks.[12-14]Asthe forward-facing jet is used alone, large mass flux of jet is needed[15]. The forward jet and spike (CFS) is the combination of the spike and the forward-facing jet. CFS can decrease the jet energy requirement with the perfect effect on drag and heat flux reduction. At the same time the cooling effect of the jet can solve the ablation problem caused by heat flux accumulated in stagnation point[16,17]. It has great potential in the development of projection.

The flow characteristics around the blunt body with CFS are complicated,the flow structure of which is showed in Fig 1. There are phenomena of bow shock, reattachment shock, recirculation vortexes, mach disk, shock wave /boundary interface, shock wave /shock wave interface etc. However, the researches on it were carried out just in recent years. The numerical investigations carried out by Geng Yunfei[13] showed that the reduction of drag and heat flux by using CFS is better than using the forward-facing jet alone. The efficiency of drag reduction and heat flux decrement with CFS is superior to that with jet only. Moreover, by increasing the nozzle diameter, the interference effects of shock wave in the shoulder-reattachment region is able to be reduced with larger amount of jet,

[1]*China Academy of Aerospace Aerodynamic,Yungangxi RD, Fengtai Dist., Beijing, China, 13611319903@163.com*
[2]*China Academy of Aerospace Aerodynamic, Yungangxi RD, Fengtai Dist., Beijing, China, weiwei_fsi@163.com.*
[3]*China Academy of Aerospace Aerodynamic, Yungangxi RD, Fengtai Dist., Beijing, China,mahandong@263.net.*
[4]*China Academy of Aerospace Aerodynamic, Yungangxi RD, Fengtai Dist., Beijing, China, qymincaaa@sina.com.*

which can meet the aim of eliminating hot spot and reducing local high heat flux. The numerical simulations by Zhang Jiang[14] showed that the function of drag and design parameters (the length of spike, the total pressure of jet and the diameter of jet outlet) was 2nd or 3rd order non-linear polynomial, and the coupling effects among design parameters were evident, especially between the diameter of jet outlet and the total pressure of jet. Furthermore, they carried out the optimization with response surface methodology, and 57.1% drag reduction was achieved with less jet flow. All these investigations were performed at the conditions that are able to establish steady flow filed. The numerical investigation carried out by Naoki et al. [18] showed that periodicity oscillation appeared at the forward shock system of CFS flow field when the jet pressure ratio was relatively low. However, the flow was found to be steady indicated by the experimental data at the same condition carried out from shock wind tunnel. They deemed that more detail experimental research ought to be carried out to understand the unsteady flow mechanism, which already emerged in the numerical simulations.

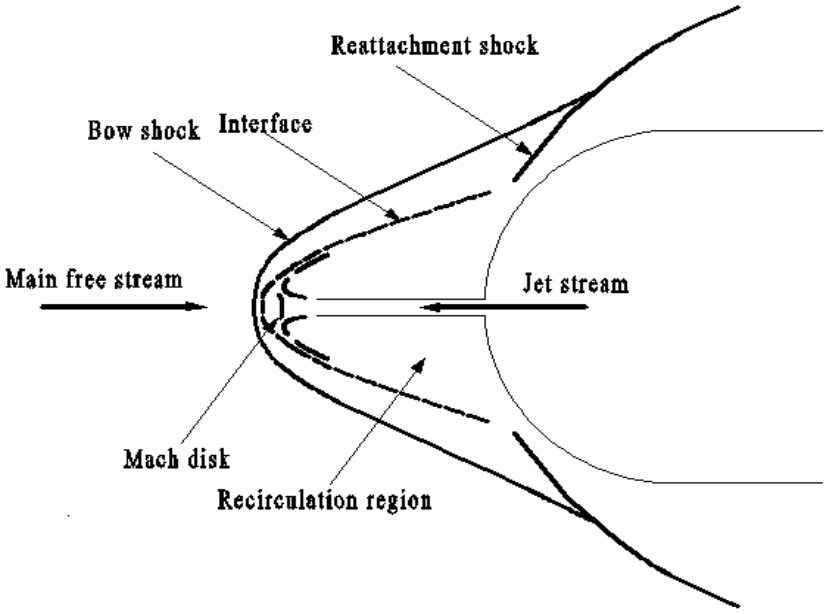

Fig 1. Sketch on the flow structure around the blunt body with CFS

The priority of former researches is on the validation about the drag and heat flux reduction effect of CFS, as well as the parameter optimization, while the study of character and mechanism on it is deficient. Numerical simulation is the primary method on the previous investigations but the experimental result is comparatively rare. Previous studies show that both stable mode and unstable mode exist in the spike or the forward-facing jet. [19-23] The regular self-excited oscillations of shock waves near the head of blunt body arose at the forward of it under the unstable mode.[24] This oscillation is induced by the forward transmission of pressure fluctuation through subsonic recirculation zone, and a critical value exists which is related to the needle length, the jet pressure ratio, or other parameters.[27-29] In addition, this kind of pressure fluctuation is caused by free shear layer or the interaction of shock wave and boundary layer. [25,26] Whether the similar flow modes occur in the CFS? And what are the flow mechanism and characteristics of CFS? These questions still need to be further investigated.

Our research focuses on the flow characteristics around CFS, which is carried out in a trisonic wind tunnel. A revolution body with the blunt nose and a CFS device on it has been researched. Fluctuating force measurement, fluctuating pressure measurement, and schlieren observation are involved. The flow characteristics of CFS in stable/unstable mode are investigated, as well as the surface pressure distributions of the blunt body, which will deepen the knowledge of the flow phenomena abovementioned further.

2. Experimental Apparatus and Model

2.1. Model Description

The configuration of the revolution body with blunt nose is shown in Fig. 2. The diameter of it is D=120mm, total length of it is L=450mm, the head of the model is hemispheroidal, and its radius is R=60mm. Spike through the hole of nose at blunt body and can be changed during the experiment. The lengths of spike tested are $L_j = 0$mm,50mm, 90mm, 100mm, 150mm, 200mm, 250mm. The nozzle exit diameter are $D_j =$ 2mm,3mm, 5mm, 10mm, 15mm, which had a convergent-divergent internal shape and the exit Mach number is 2.5. The spike located at the jet chamber of blunt body is fixed to the strut with a bracing stick. The blunt body is fixed to the balance and do not contact the spike and jet chamber. A labyrinth is designed to prevent the flow through the gap between blunt body and spike. In order to monitor the internal pressure of the model and modify the base drag, four pressure measuring tubes are installed inside the blunt body. To increase the response frequency of force measurementsystem,this model is made of aluminum alloy, which is effectively to reduce the weight.

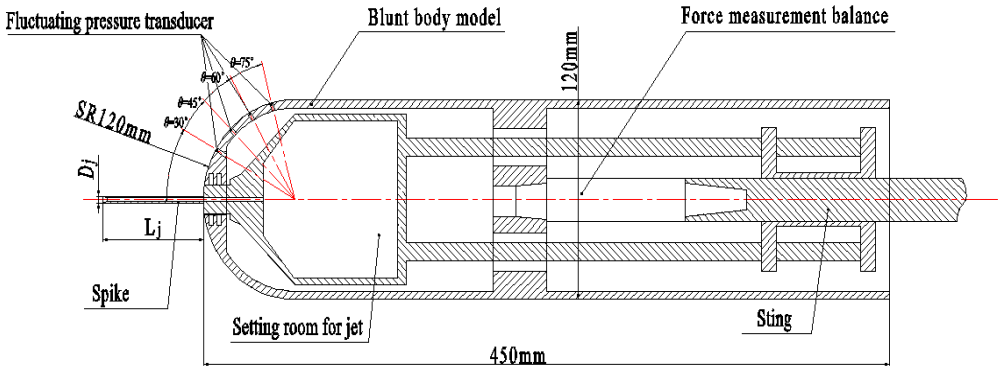

Fig 2 Sketch on the wind-tunnel model and the locations of fluctuating pressure probes

2.2. Jet Supplement System

The high-pressure gas of the jet is imported to the jet chamber by the chamber ducts, which can be regulated for different nozzle pressure ratios P_{0j}/P_{02} (the ratio of jet total pressure to shock-rear pressure of the primary flow). The range of jet total pressure is 0.1 to 20 MPa, and four high-range pressure sensors are installed in the chamber, which are utilized to monitor the real-time pressure. The jet pressure was controlled by the pressure regulation system outside the test section of the wind tunnel, later it was connected to the inlet of chamber via the high pressure flexible pipe.

2.3. Wind Tunnel and MeasurementInstrumentation

The investigation was performed in a tri-speed wind tunnel in China Academy of Aerospace Aerodynamics. The tunnel is an intermittent semi-circulation tri-sonic wind tunnel with Mach number ranging from 0.4 to 4.45. The test section is 0.6m × 0.6m, and the length of which is 1.575m. The two-dimensional nozzle section can be changed in the supersonic experiment to adjust the Mach number. Two observation windows are fixed to each side of wind tunnel, and schlieren is equipped for the flow survey.

Forces and moments on the model were measured with a self-developed six-component strain balance which features of high response frequency. Four Kulite-XCL-100 fluctuating pressure sensors whose natural frequency is 600 KHz were located at the forward of the model. The location of it and the definition of θ are shown in Fig. 2. The DH5927 dynamic test analysis system was used for the signal output of balance and fluctuating pressure sensor in the data measurement and processing, and the measurement error is less than 0.5% FS.

2.4. Experimental Parameters and Data Reduction

Experiments were carried out at the conditions of Ma=2.4 and Ma=4.0. The parameters (total pressure before the shock wave P01, total pressure after the shock wave P02 and total temperature

T0) are shown in Table 1. The total temperature of jet was 299K. The drag experimental results of blunt body were presented in the form of Cd/Cd_0. Cd_0 was measured from a single blunt body at the same condition. The fluctuating pressure results are in the normalization form, $C_p=(P-P_\infty)q_\infty$, in which P_∞ and q_∞ denotes the static pressure and dynamic pressure, respectively.

Table 1. Parameters for the main flow field of the wind tunnel

	P_{01}/MPa	P_{02}/MPa	T_0/K
Ma=2.5	0.27	0.133	289
Ma=4.0	0.58	0.078	289

3. Experimental Results and Analysis

3.1. Two Flow Modes and the Critical Condition

The experimental results indicate that both of the steady and unsteady modes exist in the flow of the CFS. Fig. s 3a) and b) are shadowgraph images of stable mode （P_{0j}/P_{02}=8.0）and unstable mode （P_{0j}/P_{02}=5.0）. With the effect of CFS, the primary bow shock detached from surface and a significant interaction occurred between the reverse jet and primary flow. A free shear layer was generated at the downstream, after whom a taper recirculation zone was formed. The interface between jet and the primary flow was unstable in the unsteady mode. The number of jet elements in the flow was more than one and the jet circulates between two flow structures. One was where jet was terminated by the primary flow in the first element and the other was terminated in the second/lateral element. For the stable mode, the forward shock waves were stable and there was only one jet element in the flow, which was terminated by the primary flow. A Mach disk was formed with a detached shock wave which is clearer than the one of unstable mode. In Fig. 3, it should be indicated that although the nozzle pressure ratio in the unstable mode is lower than the stable one, the penetration distance in the primary flow is longer than the stable one.

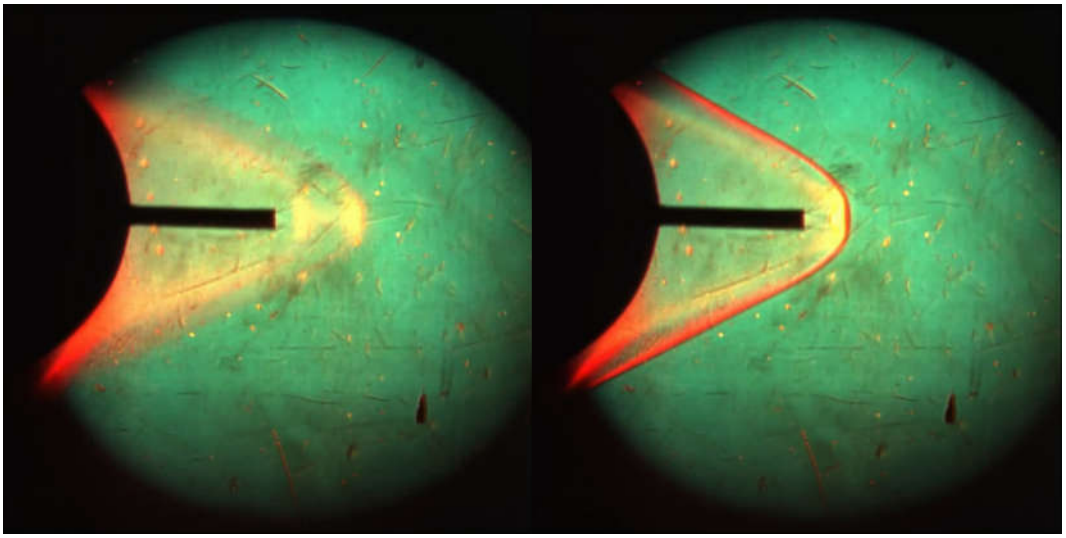

a) Stable mode, P_{0j}/P_{02}=5.0　　b)Unstable mode, P_{0j}/P_{02}=8.0

Fig 3. Shadowgraph photographs of stable mode and unstable mode, $M_a=4.0$, $L_j=50\text{mm}$

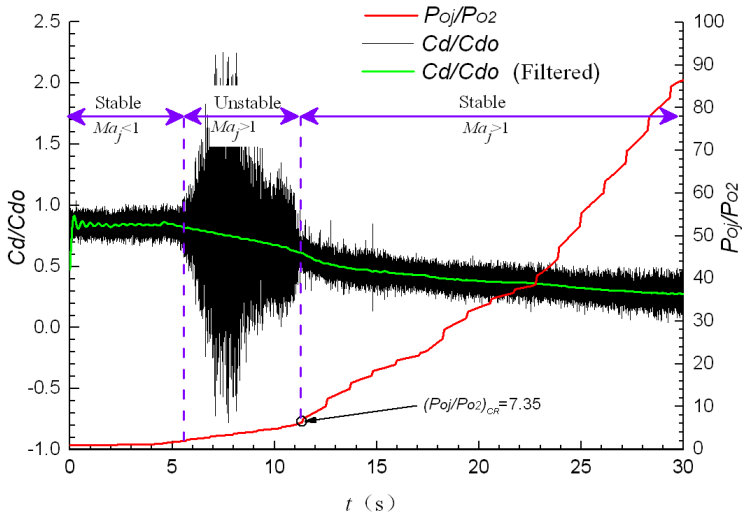

Fig4. The drag variation along with the time, $M_a = 4.0$, $L_j = 50\text{mm}$

To determine the conditions at which the unstable mode would occur, the nozzle pressure ratio was varied gradually while the primary flow was steady. Due to that the forward shock wave system fluctuates violently under unstable mode, the pressure on the blunt body would also be fluctuating intensively; therefore the drag would oscillate sharply. The variation of Cd/Cd_0 with the increasing nozzle pressure ratio was shown in Fig. 4 for free stream Mach number equals to 4.0. While $P_{0j}/P_{02} < 2.03$, owing to back pressure of incoming flow the exit of the jet was subsonic. The fluctuation of Cd/Cd_0 was not obvious and the flow was in the stable mode. The Mach number of the jet was 2.5 when P_{0j}/P_{02} was higher than 2.03 and both of the steady and unsteady modes existed in the flow. The drag of blunt body change sharply while $2.03 < P_{0j}/P_{02} < 5.72$ and the self-excited oscillations of shock waves occurred at the head of the model, thus it is the unstable mode. The fluctuation of drag disappeared when $P_{0j}/P_{02} > 5.72$, which also emerged for other working conditions, and the discrepancy was that the critical nozzle pressure ratio changed with different conditions. It was clear that P_{0j}/P_{02} is the primary factor influencing the mode of the CFS flow when the velocity of jet is supersonic and there is a critical nozzle pressure ratio $(P_{0j}/P_{02})_{CR}$, for example $(P_{0j}/P_{02})_{CR}$=5. 72 in Fig. 4. When $P_{0j}/P_{02} < (P_{0j}/P_{02})_{CR}$, the flow is in the unstable mode, while it is in the stable mode when $P_{0j}/P_{02} > (P_{0j}/P_{02})_{CR}$. The results also exemplify that the value of $(P_{0j}/P_{02})_{CR}$ was affected by the working condition, such as Mach number of primary flow, the length of spike, the diameter or shape of jet exit, and so on.

3.2. Flow Characteristics in the Stable Mode

The forward-push distance and intensity of the detached shock waves in primary flow were the primary factors that determined the pressure distribution on the blunt body and CFS flow. The pressure distribution was more sensitive to the length of spike L_j while the CFS flow was mainly determined by the nozzle pressure ratio P_{0j}/P_{02}.

The variation of drag for the blunt body with different spike length along with nozzle pressure ratio P_{0j}/P_{02} is shown in Fig. 5. The diameter of jet exit is $D_j = 2\text{mm}$ .The low-passing filtering frequency of 2.5Hz was used to reduce the effect of the fluctuation of measured signals. The drag of the blunt body with $L_j = 100\text{mm}$ was about $0.3Cd_0$ lower than that with $L_j = 50\text{mm}$. Therefore, the longer spike would push away the detached shock further, which would obviously reduce the surface pressure on the blunt body. However, there was a critical value for the spike length. When the critical value approached, the effect of pressure decrement would be reduced. For example, the drag for $L_j = 150\text{mm}$ is only $0.1Cd_0$ lower than that of $L_j = 100\text{mm}$. Due to that the spike stiffness is decreased with the increased spike length, there exists an optimal length which comprehensively considers the structure and aerodynamic design. For different spikes lengths, With the increment of P_{0j}/P_{02}, the decrease rate of the drag for the blunt body changes from fast to slow, and becomes

gentle in the end. The changes of pressure coefficient for each pressure measurement point with the increment of P_{0j}/P_{02} are shown in Fig. 6, which is validated by the variation trends of pressure for the location of $\theta = 45°$ and $\theta = 60°$.

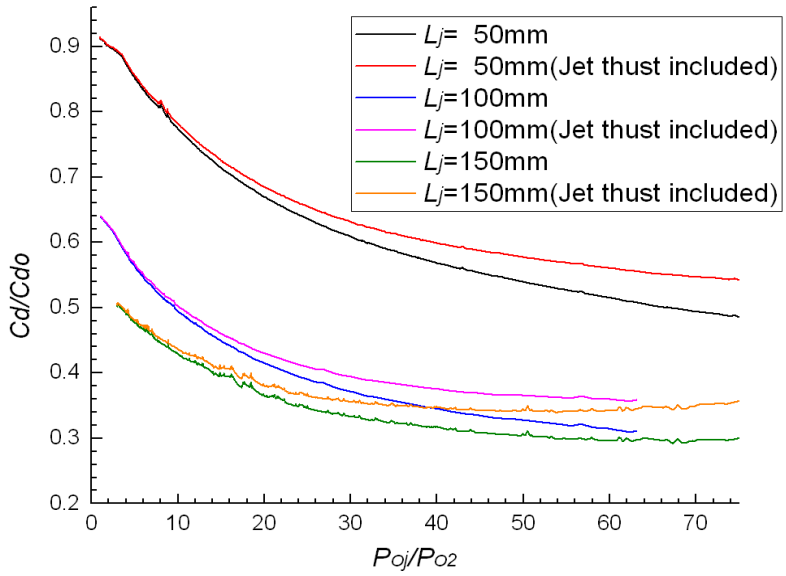

Fig 5. The variations of blunt body drag with different nozzle pressure ratio, $Ma = 4, D_j = 2\text{mm}$

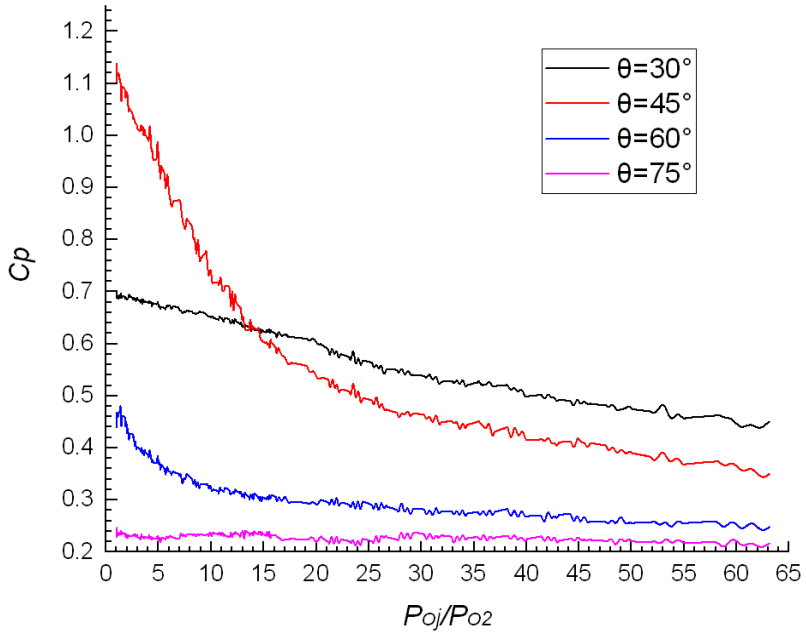

Fig 6. The variation of pressure coefficient with different nozzle pressure ratio, $Ma = 4, L_j = 100\text{mm}, D_j = 2\text{mm}$

The effects of drag reduction while increasing the nozzle pressure ratio are similar for spike length of 50mm and100mm. While for 150mm, the effect is relatively worse than shorter spike lengths. Moreover, the drag will increase slightly for $P_{0j}/P_{02} > 50$, which was caused by the increment of jet reverse thrust. Therefore, in practical application, multi-parameter optimization ought to be performed to achieve the optimum point, which is in accordance with the findings in Ref.14.

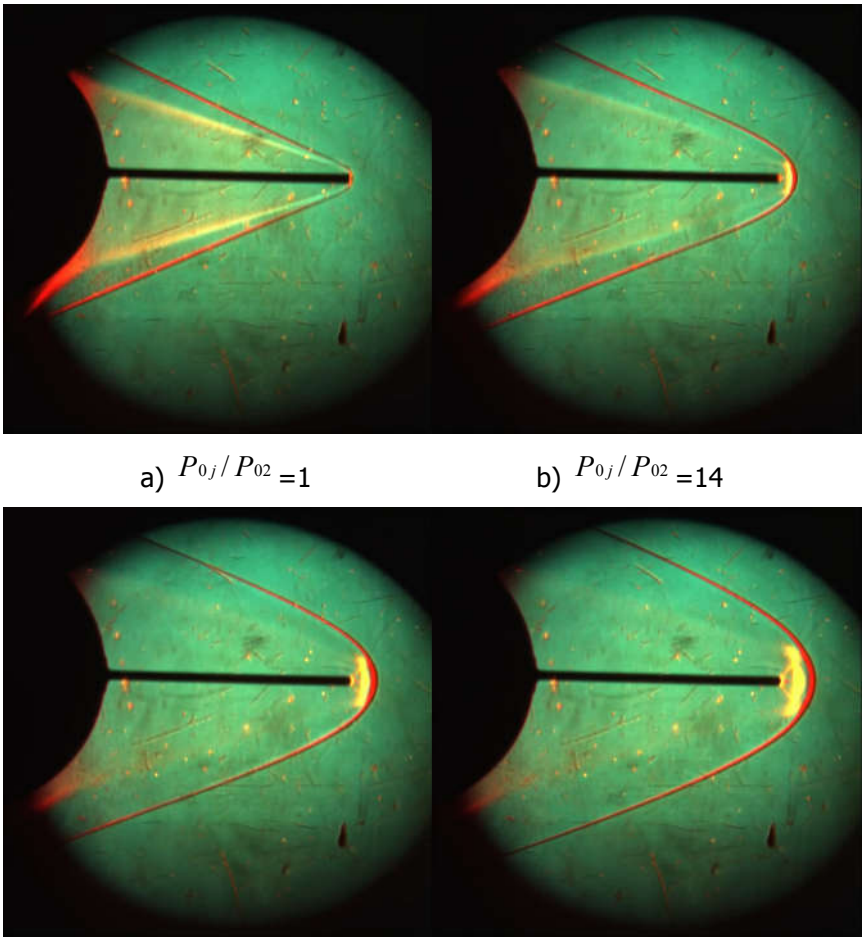

a) P_{0j}/P_{02} =1 b) P_{0j}/P_{02} =14

c) P_{0j}/P_{02} =38.3 d) P_{0j}/P_{02} =63

Fig 7. Shadowgraphs of CFS with different jet pressures, $Ma=4, L_j=100\text{mm}, D_j=2\text{mm}$

Increasing the nozzle pressure ratio is able to increase the forward-push distance of the detached shock wave, more importantly, the strength of detached shock wave can be intensified. The shadowgraphs of $L_j=100\text{mm}$ flow with different nozzle pressure ratio are shown in Fig. 7. It presents that with the increase of P_{0j}/P_{02}, the detached shock wave evolves from a approximately sharp taper to the blunt taper shape. The interface of recirculation zone and primary flow is plumped outwards and the brightness of expansion wave for the interface was attenuated. The pressure in the circulation regime is closer to the static pressure of primary flow behind the wave; in addition, the nose pressure is reduced.

Local hot spot and high pressure emerge due to the strong reattachment shock wave on the shoulder of the blunt body for single spike configuration. The numerical results in Ref.13 indicated that this shortcoming could be overcomed by additional jet, and in this paper experiments were carried out to testify this. The measuring point at $\theta=45°$ in Fig. 6 locates in the recirculation zone, and the pressure coefficient equals to 1.12 for the single spike configuration. While the jet pressure ratio is increased, the pressure is continuously decreased. For pressure ratio equals to 14, Cp equals to 0.62 at this point, which is approximate to that for $\theta=30°$ located in the recirculation regime, and the phenomenon of pressure uprush is not obvious any more. Compared with Fig. 7, it is apparent that the intensity of reattach shock wave is significantly reduced with the increment of P_{0j}/P_{02}. In consideration that the reattachment shock wave is the direct factor which generates local high pressure and hot spot, the decrement of shock intensity is effective to relieve the harmful effects of hot spot on the shoulder of blunt body.

From the schlieren, we can find that the shock structure in the stable mode was stable and clear. The measurements indicate that the fluctuating of the pressure on the nose was slight and the fluctuation intensity is the same order as that of blunt body only. The variations of fluctuating pressure

coefficient with the time in stable mode are shown in Fig. 8. The pressure fluctuation is minimum for the vertex regime ($\theta = 30°$) and expansion regime ($\theta = 75°$). For the shock reattachment regime ($\theta = 45°$ and $\theta = 60°$), the amplitude of pressure fluctuation is small, which is induced by the interaction of reattached shock wave and boundary layer. Power spectral analysis results show that the fluctuation energy was relatively small and no obvious dominant frequency emerges.

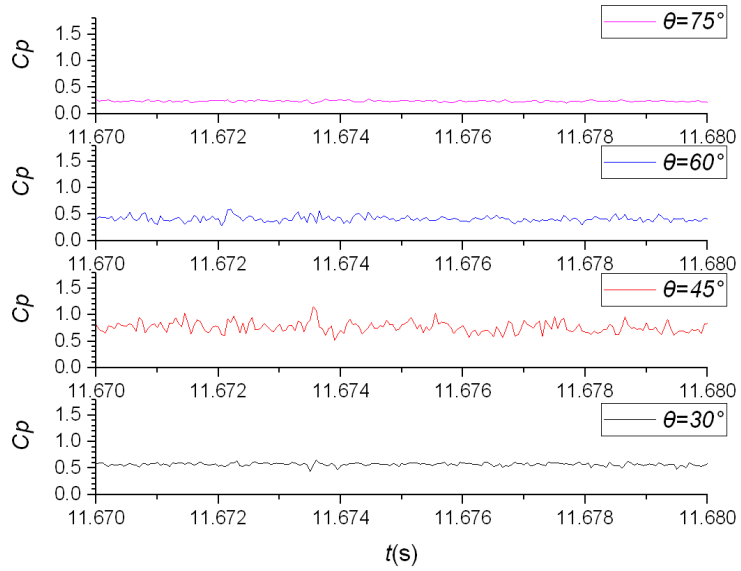

Fig 8. Fluctuating pressure coefficient of blunt body nose vs. time in stable mode, P_{0j}/P_{02} =8.0

3.3. Flow Characteristics in Unstable Mode

From the Fig. 4, we can conclude that although the fluctuation of the blunt body drag in unstable mode is severe, the filtered Cd/Cd_0 is decreased significantly with the increment of P_{0j}/P_{02}. The jet in unstable mode had a longer penetration distance in the primary flow than the one in stable mode. For a fixed penetration distance, the requirement of the nozzle pressure ratio for the jet is lower in unstable mode, which is benefit to the engineering applications. However, the shock waves at the aircraft nose oscillate significantly in unstable mode, thus the dynamic characteristics and mechanism of self-excited oscillations need to be further investigated.

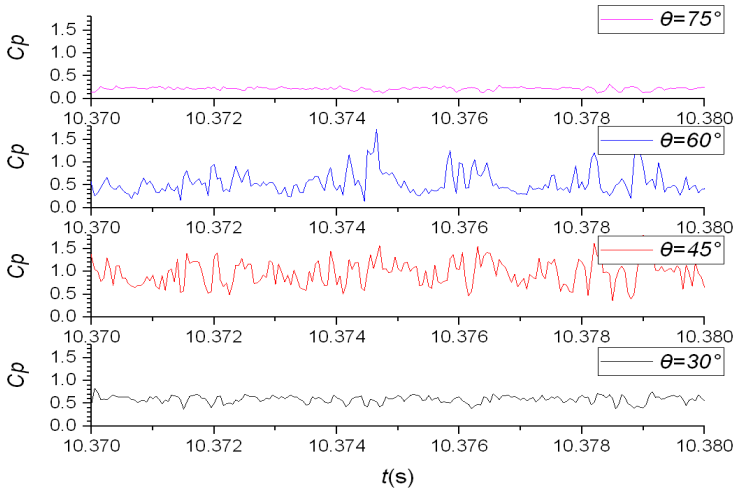

Fig 9. Fluctuating pressure coefficient of blunt body nose vs. time in unstable mode, P_{0j}/P_{02} =5.0

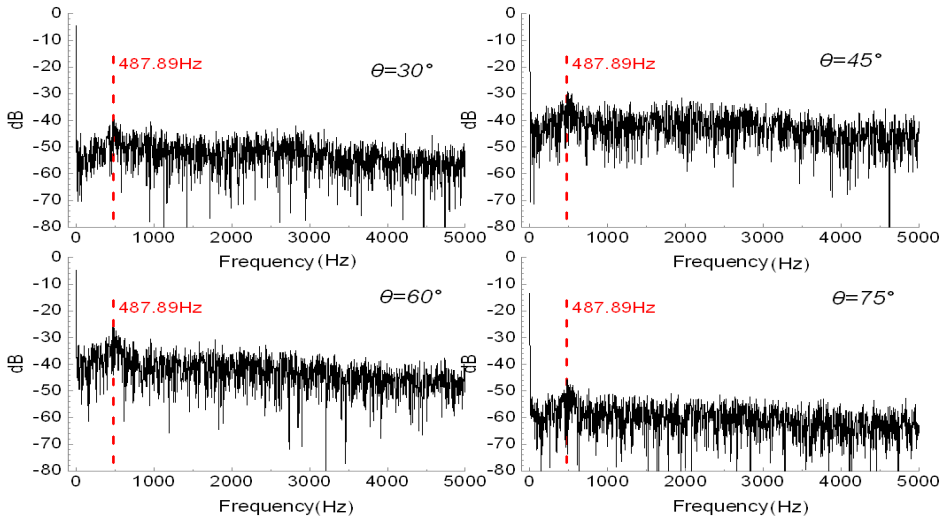

Fig10. The power spectral of fluctuating pressure in unstable mode P_{0j}/P_{02} =5.0

Fig. 9 presents the measured results of fluctuating pressure on the blunt body nose in unstable mode. Unsteady pressure fluctuation appears in the recirculation zone, which can be owed to the effects of shocks oscillation, especially the two points at $\theta = 45°$ and $\theta = 60°$. However, the magnitude of pressure fluctuation at expansion region（$\theta = 75°$）is small. Fig. 10 presents the results of the power spectral of fluctuating pressure, and the abovementioned conclusions are validated by the fluctuation intensity of each point, which reveals that the range affected by shock oscillation in unstable mode is limited. If reattachment shock wave locates in the annular regime of blunt body nose surface, the surface pressure is largely influenced by shock oscillation; while it locates in the expansion regime, the influence is significantly reduced.

Fig. 10 also indicates that the pressure fluctuation at four different locations has the same dominant frequency, $f = 487.89\text{Hz}$. The frequency spectrum analysis results show that the dominant frequency of blunt body drag fluctuation was the same under the same jet pressure ratio. We can see that in the unsteady mode, the shocks fluctuation is periodic, and possesses a definite dominant frequency. Moreover, the pressure fluctuating characteristics on the nose of blunt body are affected by it, and show the same frequency performance.

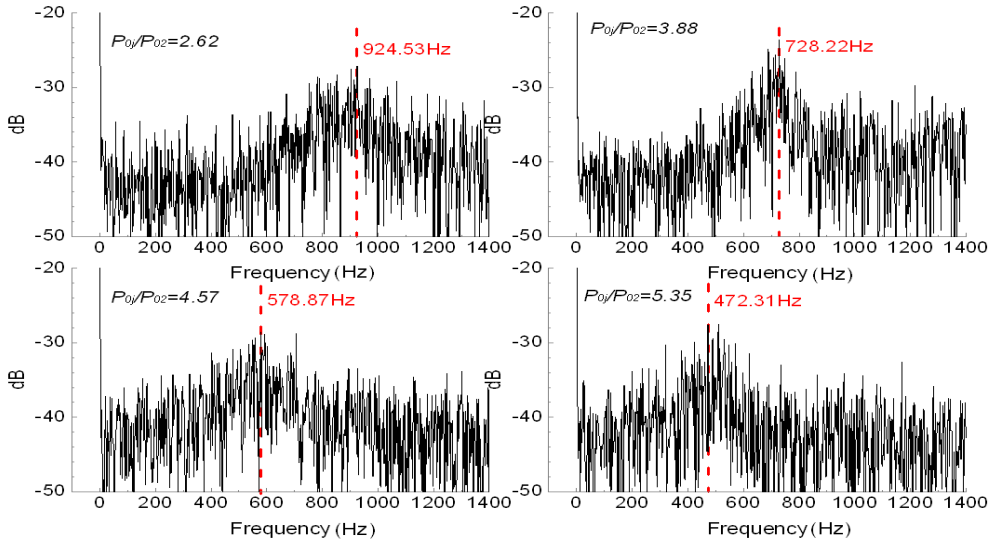

Fig 11. The power spectral of fluctuating pressure at the point $\theta = 60°$

To further reveal the relations between excitation characteristics and P_{0j}/P_{02}, Fig. 11 presents the power spectral of fluctuating pressure for different values of P_{0j}/P_{02} at the point of $\theta = 60°$. It

indicates that the dominant frequency becomes lower while increasing P_{0j}/P_{02} . There was a continuous dominant frequency range for the nozzle pressure ratio lower than the critical value (the unstable mode).

3.4. Discussion on the Driving Mechanism of self-excited Oscillations

The existent study[7] showed that the self-excited oscillation arose in the flow of blunt body with the single forward-facing jet was induced by the disturbance influence on the normal shock wave. The disturbance was transferred from the recirculation zone. There was no uniform view on the disturbance source which was from the interferer between the boundary layer and free shear layer or the reattach shocks. But the uniform view was the necessary condition of stable flow. The necessary condition was that there was only one fluidic element formatted in the jet, that's normal shock wave was generated in the jet and then was determinate by primary flow. The ejection location of jet was moved forward in the flow of CFS, and then the flow of it was similar to the single forward-facing jet. But this flow had its own obviously characteristics. The only one fluidic element generated in the jet was still the necessary condition of stable flow. The self-excited oscillation was caused for the reason that the back pressure around the jet exit had no ability to maintain a persistent balance.

The early research of Eugene S. Love [30] indicated that there was an intimate relation between the jet exit back pressure and shock reflect structures in supersonic jet. The exit shock waves had the Mach reflection at the under-expanded supersonic jet. The jet was the single element structure. But the shocks at jet exit would become a regular reflection and then several jet elements were generated when the back pressure was increased to a certain level. The position where normal shocks were terminated was located at the second or later jet elements which far away from the jet exit. The back pressure around the jet exit was $(P_d)_{CR}$ when the nozzle pressure ratio was assumed to be critical condition $(P_{0j}/P_{02})_{CR}$. The interface between the primary flow and jet would have a longer distance from the exit when $P_{0j}/P_{02} > (P_{0j}/P_{02})_{CR}$. The back pressure had a tendency of reducing in which $P_d < (P_d)_{CR}$. The jet was always the single elements structure and the flow was in stable mode. It was impossible to have a stable exit back pressure in the unstable mode. The jet shocks waves would change from mach reflection to regular reflection periodicity. The position of bow shock waves was moved front-to-back. The bow shock waves had two positions simultaneous which as seen in Fig. 3a) in the schlieren photos with a not enough exposure velocity. The self-excited oscillation was generated at the flow around the nose of blunt body.

The periodic variance of transient flow field in unstable mode is shown in Fig. 12. The Fig. 12a) presents the momentary is that the jet shock wave was Mach reflection and $P_{0j}/P_{02} < (P_{0j}/P_{02})_{CR}$. And the distance was so shorter than the critical condition when $P_d > (P_d)_{CR}$ was carried out in a flash. The jet exit shocks waves changed to regular reflection and then several jet elements were generated. As a result of this the primary was pushed farer away and the flow became the one seen in the Fig. 12b), while the multi-jet-elements were generated. Behind the bow shock waves, the interface between primary flow and jet and the shape of reattach shocks were changed respectively. The flow was completed the evolution of the one seen in the Fig. 12c). As a result of the increasing of forward-push distance, the exit back pressure was decreased and it has no ability to keep the condition $P_d > (P_d)_{CR}$. The jet exit shock waves were changed to the Mach reflection again and the flow became the one seen in the Fig. 12d). Then the jet changed to the single element again. Forward-pushed bow shock waves moved back and the flow shifted to the one seen in the Fig.12a) again. The periodic self-excited oscillation in the flow was persistent as this circle process.

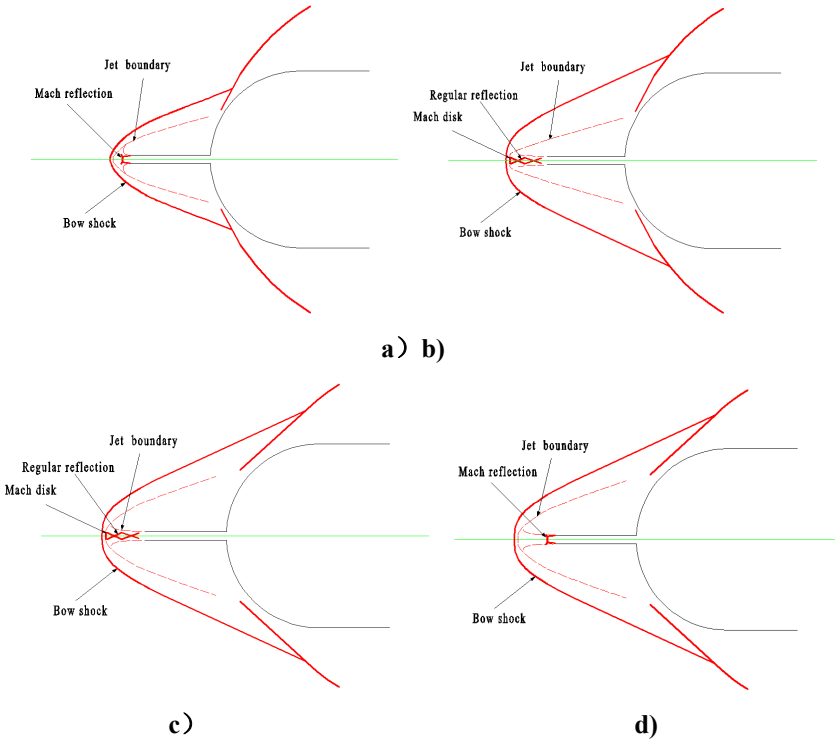

Fig12. The periodic variance of transient flow field in unstable mode

4. Conclusions

The flow performance of blunt body with the combination of forward-facing jet and spike were experimental researched in the wind tunnel. The results from this investigation have indicated the following conclusions:

1. There are stable and unstable modes in the flow field of CFS which has a critical nozzle pressure ratio $(P_{0j}/P_{02})_{CR}$. The flow is in the unstable mode when $P_{0j}/P_{02} < (P_{0j}/P_{02})_{CR}$ and in the stable mode when $P_{0j}/P_{02} < (P_{0j}/P_{02})_{CR}$.

2. The drag of the blunt body decreases with the increasing of the length of spike while the effect of drag reduction will be weakened after the length reaches a certain value. With the enhancement of jet pressure ratio, the detached shock wave evolved to the blunt taper shape and the strength of the reattach shocks is diminished.

3. The shocks fluctuation was periodic with a definite dominant frequency in the unsteady mode. The dominant frequency of the self-excited oscillation decreases with the increasing of nozzle pressure ratio.

4. The self-excited oscillation was caused for the reason that the ambient pressure around the jet exit cannot be persistently balanced at the condition $P_{0j}/P_{02} < (P_{0j}/P_{02})_{CR}$.

References

1. Hutt G R, Howe A J. Forward facing spike effects on bodies of different cross section in supersonic flow. Aeronautical Journal, 93(926): 229-234 (1989)
2. Feng Jiabo, Zhang Jiang. Drag Reduction for the Forward-facing Spike on the Blunt Nosed researching via CFD and Wind Tunnel Experiments. Fourth session of the national hypersonic aerodynamics/heat Symposium Proceedings. Wenzhou: 2007:10-13 (2007)
3. M. Y. M. Ahmed and N. Qin, Surrogate-Based Multi-Objective Aerothermodynamic Design Optimization of Hypersonic Spiked Bodies, AIAA JOURNAL, 50(4):797-810 (2012)
4. Pei Qiang. Trident missile's air cone for drag reduction. Modern military, 1985.1:23-29.
5. M Gauer, APaull. Numerical Investigation of a Spiked Blunt Nose Cone at Hypersonic Speeds. Journal of spacecraft and rockets,45(3): 459-471 (2008)

6. Meyer B, Nelson H F, Riggins D W. Hypersonic drag and heat-transfer reduction using a forward-facing jet. Journal of Aircraft,38(4): 680-686 (2001)
7. Yamauchi M, Fujii K, Higashino F. Numerical investigation of supersonic flows around a spiked blunt body. Journal of Spacecraft and Rockets, 32(1): 32-42 (1995)
8. Finley P J. The flow of a jet from a body opposing a supersonic free stream[J]. Journal of Fluid Mechanics, 26(02): 337-368 (1966)
9. He Kun, Chen Jianqiang, Dong Weizhong. Penetration mode and drag reduction research in hypersonic flows using a counter-flow jet. ActaMechanicaSinica, 38（4）：438-445(2006)
10. EswarJosyula, Mark Pinney and William B. Blake. Applications of a Counterflow Drag Reduction Technique in High-Speed Systems. JOURNAL OF SPACECRAFT AND ROCKETS,39(4):605-614 (2002)
11. R. C. Mehta. Numerical Heat Transfer Study over Spiked Blunt Bodies at Mach 6.8. J. SPACECRAFT, 37(5):700-703 (2000)
12. Jiang Wei, Yang Yunjun, Chen Hewu. Investigations on aerodynamics of the spike-tipped hypersonic vehicles. Journal of Experiments in Fluid Mechanics, 25(6): 28-32 (2011)
13. R C Mehta. Heat Transfer Analysis over Disc and Hemispherical Spike Attached to Blunt-Nosed Body at Mach 6, AIAA-2011-2228 (2011)
14. G R Srinivasan, R R Chamberlain. Drag Reduction of Spiked Missile by Heat Addition, AIAA-2004-4714 (2004)
15. Josyula E, Pinney M, Blake W B. Applications of a counterflow drag reduction technique in high-speed systems. Journal of spacecraft and rockets, 39(4): 605-614 (2002)
16. GENG Y F，YAN C, Numerical investigation on drag and heat—transfer reduction using combined spike and forward facing jet method.ActaAerodynamicaSinica, 28(4):436-440 (2010)
17. Zhang J,PengC,Cai C F,et al. Optimization research on combination of spike and forward-facing jet using response surface methodology[J].ActaAerodynamicaSinica, 33(2)：204-210 (2015)
18. Naoki Morimoto, Jang Yeol Yoon, Shigeru Aso, Yasuhiro Tani. Reduction of Aerodynamic Heating with Opposing Jet through Extended Nozzle in High Enthalpy Flow，AIAA 2014-0705 (2014)
19. Shang J S, Hayes J, Wurtzler K. Jet-spike bifurcation in high-speed flows, AIAA-00-2325 (2000)
20. Shang J S, Hayes J, Wurtzler K. Flow Oscillations of Spike-Tipped Bodies, AIAA JOURNAL, 20(1):25-26 (1982)
21. WladimiroCalarese and Wilbur L. Hankeyt. Modes of Shock-Wave Oscillations on Spike-Tipped Bodies. AIAA JOURNAL, 23(2):185-192 (1985)
22. J.P. Reding, R.A. Guenther and D.M. Scale Effects on the Fluctuating Pressures in a Region of Spike-Induced Flow Separation. AIAA-79-0143 (1979)
23. Daniel Feszty, Ken J. Badcock, and Bryan E. Richards. AIAA JOURNAL, 2004, 42(1):95-106.
24. G. Jagadeesh, M. Viren and K. P. J. Reddy. Hypersonic buzz phenomenon on the spiked blunt cones. 41st Aerospace Sciences Meeting and Exhibit, Reno, January 6-9 (2003)
25. N.D. Malmuth, Influence of a counterflow plasma jet on supersonic blunt body pressures. AIAA-99-4883 (1999)
26. Masahiro Fujita. Axisymmetric Oscillations of an Opposing Jet from a Hemispherical Nose. AIAA JOURNAL, 33(10):1850-1856 (1995)
27. W. Calarese and W.L. Hankey. Modes of Shock Wave Oscillations on Spike-Tipped Bodies. AIAA-83-0544 (1983)
28. R.A. Guenther and J.P. Reding, Fluctuzting Pressure Environment of a Drag Reduction Spike. AIAA-77-90 (1977)
29. W. Calarese and W.L. Hankey, Modes of Shock Wave Oscillations on Spike-Tipped Bodies, AIAA-83-0544 (1983)
30. Love Eugene S, Grigsby Carl E, Lee Louise P, Woodling Mildred J. Experimental and Theoretical Studies of Axisymmetric Free Jets, NASA-TR-R-6 (1955)